2-D Finite Difference Modeling of Microwave Heating in the Prostate

David Y. Yuan[1], Jonathan W. Valvano[1], Eric N. Rudie[2], and Lisa X. Xu[3]

[1] Biomedical Engineering Program, University of Texas, Austin, Texas

[2] Urologix Inc., Minneapolis, Minnesota

[3] Dept. of Applied Sciences, College of Staten Island, Staten Island, New York

Abstract

Accurate prediction of temperatures in the prostate undergoing thermally-based treatments is crucial to assessing efficacy and safety. A two-dimensional transient finite difference model for predicting temperatures in prostate undergoing microwave heating via a transurethral fluid-cooled catheter is presented. Unconditional stability and good accuracy are achieved by using the alternating direction implicit method. A transverse section of the prostate centered at the urethra is modeled in cylindrical coordinates. The model geometry consists of a hollow silicone cylinder, representing the catheter, surrounded by multiple regions of tissue. Cold fluid flowing through the catheter minimizes the temperature in the periurethral tissue. This flow is modeled as a convective boundary condition at the surface between the catheter lumen and wall. The outer surface of the tissue is assumed to remain at baseline temperature. Microwave heating has both a radial and angular dependence. In order to maximize the heat to the target tissue, the microwave field emitted from the transurethral catheter focuses heat away from the rectum. Different perfusion situations within the prostate are simulated. Pennes' perfusion term is assumed to model the effect of perfusion on heat transfer. Results of the numerical model are compared to phantom experiment results. The model parameters which provided the best fit for the phantom was extended to model canine prostate.

Nomenclature

A	microwave power parameter [W]
c	specific heat [J/kg-˚C]
d	microwave power offset factor [m]
h	convective coefficient [W/m^2-˚C]
k	thermal conductivity [W/m-˚C]
q''	power flux due to microwave heating[W/m^2]
q'''	volumetric microwave power [W/m^3]
r	radial position [m]
Rs	catheter diameter [m]
Rt	tissue diameter [m]
s	offset of microwave antenna from geometric center [m]
T	temperature [˚C]
β	microwave attenuation constant for uniform plane wave [m^{-1}]
ω	blood perfusion rate [m^3/m^3-sec.]
θ	angle [radians]
ρ	density [kg/m^3]

Subscripts:

a	arterial
b	blood
c	convective
i	inner
o	outer
t	tissue
s	silicone (catheter)
c	cold water (within catheter)

I. Introduction

The treatment of benign prostatic hyperplasia (BPH) has implications which affect the majority of the adult male population. Pathologic BPH is observed in approximately 50% of elderly men in their sixth decade, and the incidence increases to almost 100% by the eighth decade [1]. About half of these men will develop macroscopic enlargement of the gland, and clinical signs and symptoms will be manifested in about half of this population. Although benign compared to prostate cancer, clinical symptoms can dramatically alter the quality of life. The hyperplastic tissue can cause constriction of the urethra and thus affect voiding of urine. Factors to consider for thermally-based treatments of the prostate include minimization of thermal injury to the urethra and rectum, and maximal delivery of thermal energy to target tissue. Minimizing temperature rise in the urethra allows for minimal or no anesthesia, and is believed to reduce post-operative complications. Protection of the rectal wall is especially important since injury can lead to clinical complications as severe as a rectal fistula. Due to its location immediately dorsal to the prostate, the ventral aspect of the rectal wall is susceptible to overheating when a uniform radiating microwave heat source is applied transurethrally to treat the prostate.

The Urologix® Transurethral Thermal Therapy (T3®) system addresses the need for protection of the urethra and rectum from thermal injury. Its objective is to thermally necrose the hyperplastic tissue using controlled microwave energy to decrease constriction of the urethra. Microwave energy is delivered via a transurethral catheter with cold water flowing through subsurface lumens. The cold water flow minimizes temperature rise in the periurethral tissue which is located immediately adjacent to the catheter. The T3® catheter delivers energy to the prostate such that heat generation is greater towards the ventral and lateral aspect of the prostate and minimal towards the dorsal aspect. This is achieved by altering the shape of the microwave field by the catheter lumen configuration. Thus, higher temperatures can be achieved in the tissue of interest than can be achieved from uniform radiating catheters.

This paper presents the extension of the one dimensional time dependent model developed by Xu, Rudie, and Holmes [2] to two dimensions. The model represents the two dimensional transverse cross section of the prostate. Catheter parameters derived by Xu *et al.* were adjusted so that model temperatures fit those measured in the phantom. These parameters were then used to perform parametric studies which include the study of perfusion using Pennes' model [3]. The new model is implemented using alternating difference implicit finite difference method [4] . The finite difference approach was adopted over the finite element method due to the lower development cost and the simple model geometry.

II. Methodology

A. Experimental Gel Phantom Studies

Phantom experiments were performed in tissue-equivalent polyacrylamide gel prepared as described by Xu *et al.* [2]. The T3 catheter was placed in the center of the gel with sufficient surrounding gel to assume a constant temperature boundary condition. Fiber optic Luxtron® temperature probes were situated within the gel 180˚ apart and were aligned with the angular position where maximum and minimum microwave heat generation occur (Figure 1). As shown in the figure, the probes measuring the

higher temperatures would correspond to the ventral region in the prostate and are labeled as the ventral probes. Likewise, the cooler temperatures are measured by the dorsal probes. In addition to the probe temperatures, both microwave power and coolant temperature were also sampled every five seconds.

B. Model Formulation and Assumptions

1. Governing Equations and Model Geometry

To model the effect of perfusion, Pennes' bioheat equation was used. In cylindrical coordinates, the volumetric heat generation from metabolism is replaced by that from a microwave source, and the equation takes the form

$$(\rho c)_t \frac{\partial T_t}{\partial t} = \frac{1}{r}\frac{\partial}{\partial r}\left(k_t\, r \frac{\partial T_t}{\partial r}\right) + \frac{1}{r}\frac{\partial}{\partial \theta}\left(\frac{k_t}{r}\frac{\partial T_t}{\partial \theta}\right) + (\rho c)_b \omega_b (T_a - T_t) + q''', \quad r > Rt_i$$

Within the catheter, microwave heat generation is neglected, and the heat transfer is simply

$$(\rho c)_s \frac{\partial T_s}{\partial t} = \frac{1}{r}\frac{\partial}{\partial r}\left(k_s\, r \frac{\partial T_s}{\partial r}\right) + \frac{1}{r}\frac{\partial}{\partial \theta}\left(\frac{k_s}{r}\frac{\partial T_s}{\partial \theta}\right), \quad Rs_i \le r \le Rs_o$$

The boundary conditions are

$$-k_s \frac{\partial T_s}{\partial r} = h_c (T_s - T_c) \qquad \text{at } r = Rs_i$$

$$k_t \frac{\partial T_t}{\partial r} = k_s \frac{\partial T_s}{\partial r} \qquad \text{at } r = Rs_o$$

$$T_t = 24.5\ ^\circ C \qquad \text{at } r = Rt_o$$

Initially, the model temperatures are uniform at 24.5 ˚C. A constant temperature boundary condition corresponding to the initial temperature is imposed at the outer tissue boundary. Cold water flow through the catheter is modeled as a convective boundary condition at the catheter inner surface.

The transverse cross-section of the prostate was represented as a circle with the urethral catheter located at the center (Figure 2). Based on symmetry of the left and right lateral lobes of the prostate, the model reduces to that of a semicircle. The model is comprised of three regions: the inner most region is the catheter, followed by the prostate tissue, and then the peripheral tissue at the outermost region. The catheter cross-sectional geometry is assumed to be a circle, and subsurface catheter lumens are modeled as a single lumen. Within the prostate tissue, two regions of perfusion can exist as proposed by Xu *et al.* [2]. The rectal wall adjacent to the prostate is represented by the portion of the peripheral tissue dorsal to the prostate.

2. Model Parameters

a. Catheter, Phantom, and Tissue Properties

Properties pertaining to the model for phantom gel, tissue, and catheter are provided. Thermal properties for silicone were used for the catheter. Thermal properties for the phantom gel were identical to those used by Xu *et al.* [2]. Values measured in the canine prostate by Yuan *et al.* [5] were used for the thermal properties of the prostate. Microwave heat generation in the catheter was neglected and the microwave attenuation constants (β) used for tissue and phantom gel was 41.284 m^{-1} [6]. Values for prostate perfusion were based on perfusion measurements in canine prostates by Andersson *et al.* [7]. Arterial temperature was assumed to be at 37 ˚C. The properties are summarized in table 1.

b. Microwave Heat Generation in Tissue

Formulation of the microwave heat generation by Xu *et al.* [2] was extended to include an angular dependence term. The preferential heating of the microwave source was modeled by an offset (d) from geometric center of the microwave antenna and an angle dependence. Angle dependent attenuation was derived from the eccentricity of the microwave antenna. The near field cylindrical electromagnetic field power flux can be described by

$$q''(r,\theta) = A\frac{e^{-\beta(r-s\cos\theta)}}{r - s\cos\theta}$$

where A_t is a linear factor relating to the microwave antenna power determined by temperature mapping [2], and β is the attenuation constant for an uniform plane wave in a given media.

The volumetric heat generation is then given by

$$q'''(r,\theta) = -\frac{1}{r}\frac{d}{dr}\left(r q''(r,\theta)\right) = A\frac{e^{-\beta(r-s\cos\theta)}\left(s\cos\theta + r\beta(r - s\cos\theta)\right)}{r(r - s\cos\theta)^2}$$

This equation limits the maximum value for the offset (s) beyond which negative q''' will result. An example of the volumetric heat generation distribution within the model is shown in figure 3. The heating protocol used for the model are ramp changes in microwave power over time as shown in figure 4.

c. Convective Coefficient

The convective coefficient obtained by Xu *et al.* was used as an initial estimate. Even though the temperature and the overall flow velocity of the cold water flow within the catheter were measured, a reliable convective coefficient was difficult to obtain due to the catheter design. This parameter was adjusted to 127.5 W/m^2-˚C so that an acceptable fit to experimental phantom temperatures could be obtained. The process for arriving at the desired parameters so that model predictions fit those of the phantom are described next.

4. Adjustment of parameters to fit phantom results

Two parameters for which the measurements were unavailable were adjusted to minimize temperature differences between the model results and phantom experiments. Iterations were performed using different values of the antenna power factor (A) and the convective coefficient (h_c) until acceptable temperature errors were obtained. The search criteria evaluated the mean squared error of the radial temperatures associated with the probes. The average of the mean squared error of the ventral and dorsal probes was then calculated to derive the subsequent set of parameter values to search. These values were obtained at selected points in time so as to evaluate the error over the simulation period.

5. Assumptions

Assumptions used in the preceding development of the model are summarized. Geometrically, the transverse cross-section is modeled as a circle with the urethral catheter located at the center. The catheter cooling effect is modeled by a lumped constant convective coefficient. Microwave heat generation in the catheter is assumed to be negligible. The rectal wall is modeled as part of the peripheral tissue with the same properties as the prostate. Temperature at the outer boundary of the peripheral tissue is assumed to remain at baseline. Perfusion was modeled using Pennes' term. Perfusion was assumed to be uniform within a distinct perfusion region and the arterial temperature was assumed to be constant. Thermoregulatory response was neglected. Changes to tissue thermal properties and perfusion caused by thermal damage was also not modeled.

C. Numerical Implementation

Alternating direction implicit (ADI) finite difference method [4] was used to numerically implement the model. This method removes the restriction on time step and model mesh imposed by the stability criteria of the explicit approach. Discretization was performed by applying the energy volume average within each quadrant surrounding the node of interest. The development follows that described by Qi and Wissler [8]. Grid size within the tissue increased with increasing radial distance from the catheter since higher temperature gradients were expected near the catheter. The heating protocol was implemented by using an input data file which contains the microwave power sampled every 5 seconds. This input file also includes the variation in coolant temperatures.

III. Results

A. Without Perfusion

Results which show the accuracy of the model to the phantom gel and the sensitivity of the model to thermal properties are presented. The transient temperature profile development of the phantom model using properties shown in table 1 is shown by figure 5. Peak temperatures occur beyond the catheter and decrease in the angular as well as the radial direction. Initially (time 205 and 605 sec. of figure 5), temperatures of the inner region is lower than baseline due to the convective cooling of the catheter. To illustrate the preferential heat generation of the catheter, the temperature contours at 1405 seconds (microwave power = 20 W) are plotted in figure 6. Model temperatures at

sensor locations of the ventral and dorsal probes within the phantom gel were compared in figures 7, 8, 9 and 10 to assess the accuracy of the model prediction. Temperature profiles along the radial direction of the ventral and dorsal probes at 200 second intervals are plotted in figures 8 and 9, respectively. The difference between the measured and predicted temperatures for both the ventral and dorsal probe locations are shown in figures 9 and 10, respectively.

The sensitivity of model temperatures to thermal properties is shown figure 11. The model was run with prostate thermal properties (Table 1),

k = 0.56 W/m-˚K, ρ = 1000 kg/m^3, and c = 4175 kJ/kg-˚C, and

k = 0.5 W/m-˚K, ρ = 1000 kg/m^3, and c = 4175 kJ/kg-˚C.

The alternative thermal properties were chosen because they represent typical values for gel and blood. The temperature differences shown occur along the ventral probe location at the end of the heating protocol.

B. With Perfusion

1. Single Perfusion

A range of perfusion was simulated to study the effect of Pennes' perfusion term on model temperature. Based on values measured in canine prostate by Andersson *et al.* [7], perfusion values of 10, 30, 50, 70, and 90 ml/100g-min. were chosen to represent the possible range of perfusion within the prostate. Andersson *et al.* found perfusion values to range from 31 to 79 ml/100g-min using the Xe^{133} clearance technique. Assuming the perfusion within the prostate to be one constant uniform value, the model temperatures for different perfusion at the end of the heating protocol are shown in figure 12. These radial temperature profiles coincide with the location of the ventral probe. The effect of preferentially heating the ventral aspect of a perfused prostate is shown by the difference between temperatures at the ventral and dorsal probe location in figure 13. To analyze the influence of perfusion on the prediction of temperature, the temperature difference between the models with the two extreme perfusion values of 90 ml/100g-min. and 10 ml/100g-min. is shown in figure 14. This can be interpreted as the worst case in erroneously assuming a perfusion value within the canine prostate. To study the sensitivity of the temperature error when the assumed values of the perfusion differ by 40 ml/100g-min, three perfusion ranges (90 and 50, 70 and 30, and 50 and 10 ml/100g-min) were also compared at 1605 seconds (Figures 15). These temperature differences are along the radial location coinciding with the ventral probe location at the end of the heating protocol.

2. Two Region Perfusion

Based upon the analysis of Xu *et al.* [2] and prostate perfusion measurements by Yuan *et al.* [9], studies of models with more than a single uniform perfusion were performed. Xu *et al.* presented the model of having higher perfusion within the periurethral zone, which was modeled as the inner 25% of the prostate. Using microspheres, Yuan *et al.* measured the perfusion to be lower in the periurethral region of the canine prostate. A model assuming the lower perfusion for the inner region to be 30 ml/100g-min., and the outer region, as well as the peripheral tissue, to be 70 ml/100g-min. was compared to the uniform 50 ml/100g-min. perfusion model. The inner perfusion region was designated to be from the radial position 2.5 mm to 6.25 mm based on general histological observations. This is approximately the inner 25 % of the prostate. The temperature difference between these two models is shown in figure 16. Two models with continuous linearly changing perfusion were also studied. Perfusion for one model increases linearly from 30 to 70 ml/100g-min. with radial position, while the other decreases with radial position. Figure 17 shows the difference in temperature between the linearly varying (30 to 70 ml/100g-min.) and the single perfusion model (50 ml/100g-min.), the linearly varying and the two distinct perfusion region model (for perfusion values of 30 and 70 ml/100g-min.), and the two different linearly varying models. The results coincide with the ventral probe location, 1405 seconds into the heating protocol.

IV. Discussion

A. Comparison to Phantom Experiments

The results obtained from the phantom model illustrate the T3® catheter function, provide a measure of model accuracy, and evaluate model sensitivity to thermal properties. Two features of the T3® catheter are indicated in the phantom model temperature maps (Figures 5 and 6). One feature is the difference in temperature between the dorsal direction and ventral direction. From figures 7 and 8, the temperature difference between the ventral and dorsal probe locations at approximately the 1 cm radial position is about 10 ˚C. The second feature is the shift of the maximum temperature beyond the catheter outer surface into the phantom. Figures 7 and 8 show maximum temperature error to be approximately ± 3 ˚C for a temperature rise of over 25 ˚C. The underestimation at the gel outer boundary indicates the inadequacy of applying a baseline temperature Dirichlet boundary condition for the given heating protocol. Comparison of the model temperatures resulting from using different thermal properties (Figures 11) shows that assuming the thermal properties of blood in place of prostate thermal properties to be a good estimate. However, using the thermal properties of gel produces temperature predictions with errors which would be unacceptable for applications utilizing temperature increases in the range of 10 ˚C.

B. Effect of Perfusion

Sensitivity of temperature to perfusion is indicated for model runs using perfusion values similar to that for the canine prostate. Figures 12, 13, 14, and 15 show that for constant heating power, the desired temperatures may not be obtained within the prostate when perfusion is not considered. For the same heating protocol, temperature differences can be greater than 10 ˚C between perfusion of 10 ml/100g-min. and 90 ml/100g-min.(Figure 14). Thus, assuming the perfusion to be 10 ml/100g-min. when the actual perfusion is 90 ml/100g-min., results in achieving a peak temperature of only 60 ˚C as opposed the expected 70 ˚C under the 10 ml/100g-min. assumption. This underestimation over the duration of the treatment would reduce the expected therapeutic efficacy. Initially, the positive temperature differences obtained at earlier times (curves at time 405 and 805 seconds) when comparing temperatures at higher perfusion to those at lower perfusion may appear to be in error. This characteristic is due to the arterial temperature of the Pennes perfusion term being higher than baseline tissue temperature and the catheter water temperature. At earlier times, Pennes' term for tissue perfusion becomes a heat source as opposed to a heat sink. This effect is also shown in the peripheral tissue at later times (curves at time 1205 and 1605 seconds). Figure 15 shows that the effect of erroneous perfusion assumptions on temperature prediction to be less at higher perfusions. In applying the same heating protocol under circumstances where the assumed and the actual perfusion differs by 40 ml/100g-min., the resulting temperature difference is lower when perfusion is high. When the assumed perfusion is 10 as opposed to 50 ml/100g-min., and both underestimate the actual perfusion by 40 ml/100g-min., the resulting temperature within the prostate is about 8 ˚C lower as opposed to 4 ˚C. The higher temperature difference at lower perfusion points to the need for careful consideration of the perfusion variation in tissue with low perfusion.

Replacing the single perfusion model with non-uniform perfusion models using Pennes' perfusion term did not produce any substantial differences. The temperature differences in figure 16 and 17 show that replacing a single lumped perfusion (50 ml/100g-min.) model with non-uniform perfusion (30 ml/100g-min. to 70 ml/100g-min.) models results in differences of less than approximately 3 ˚C for a temperature rise of approximately 25 ˚C. In comparison, Xu *et al.* [2] obtained a good fit with experimental results using Pennes' perfusion term with the inner perfusion being at least 15 times that of the outer perfusion. The difference between the two perfusions used by Xu *et al.* exceeds the perfusion difference modeled in this paper.

Perfusion was modeled in this paper using Pennes' perfusion term and reflected those for canine prostate under normothermic conditions. With the modeled heating protocol, perfusion can be expected to exceed the range of normal perfusion used in this paper and a thermoregulatory response will also alter

perfusion dynamically. Detailed knowledge of the prostate vessel architecture, perfusion, and thermoregulatory response is necessary to justify the choice of the thermal model for perfusion. Moreover, experimental *in vivo* verification should be used to evaluate the model.

V. Conclusions

A transient two-dimensional finite difference model has been developed to predict temperatures of a prostate transverse section subject to microwave heating from a transurethral catheter. This model predicted temperatures of a tissue-equivalent phantom gel for microwave heating to within ± 3.5 ˚C over a 20 ˚C to 40 ˚C temperature rise. Using the catheter parameters which produced the best temperature fit in the phantom, the model was extended to study the temperature distribution for the prostate. The preferential heating design of the catheter was demonstrated by the non-uniform temperature distribution. Sensitivity to thermal properties was studied by running the model with the thermal properties of blood and the thermal properties of phantom gel. Substituting the thermal properties of blood for prostate resulted in temperature differences of less than 1 ˚C, whereas substituting gel phantom thermal properties produced differences of about 4.5 ˚C. Studies of the effect of perfusion, based upon Pennes' perfusion term, indicated the importance of accounting for the magnitude of perfusion within tissue. For the same heating protocol, the influence of perfusion can result in temperature differences as high as 10 ˚C. Non-uniform perfusion models were also studied and compared to the conventionally used single perfusion model. The resulting temperature differences for a non-uniform perfusion ranging from 30 to 70 ml/100g-min and a single 50 ml/100g-min. perfusion throughout the tissue indicate that a lumped average perfusion can be used with no substantial difference in predicted temperatures.

VI. References

[1] J.T. Isaacs, and D.S. Coffey, "Etiology and Disease Process of Benign Prostatic Hyperplasia," *The Prostate Supplement*, 2: 33-50, 1989.

[2] L.X. Xu, E. Rudie, and K.R. Holmes, "Transurethral Thermal Therapy (T3) for the Treatment of Benign Prostatic Hyperplasia (BPH) in the Canine: Analysis Using Pennes Bioheat Equation," *Proc. ASME Winter Annual Meeting*, HTD-Vol. 268: 31 - 40, 1993.

[3] H.H. Pennes, "Analysis of Tissue and Arterial Blood Temperatures in Resting Forearm," *J. Appl. Physiol.*, 1: 93-122, 1948.

[4] Peaceman, D.W., and Rachford, H.H., "The Numerical Solution of Parabolic and Elliptic differential Equations," *J. Soc. Ind. Appl. Math.*, 3: 28 - 41, 1955.

[6] Andreuccetti, D., Bini, M., Ignesti, A., Olmi, R., Rubino, N., and Vanni, R., "Use of Polyacrylamide as a Tissue-Equivalent Material in the Microwave Range," *Trans. Biomed. Eng.*, 35(4): 275 - 277.

[7] Andersson, L., Dahn, I., Nelson C., and Norgren, A., "Method for Measuring Prostatic Blood Flow with Xenon^{133} in the Dog," *Invest. Urology*, 5(2): 140-148, 1967.

[8] Qi, Y., and Wissler, E.H., "A Combined Analytical/Finite Difference Technique for Analyzing Two-Dimensional Heat Transfer in Human Limbs which contain Major Arteries and Veins," ASME, *Proc. ASME Winter Annual Meeting*, HTD-Vol. 231: 57 - 64, 1992.

[9] Yuan, D.Y., "Measurement of Canine Prostate Perfusion using Microspheres," unpublished data.

[10] Yuan, D.Y., Valvano, J.W., and Anderson, G.T., "Measurement of Thermal Conductivity, Thermal Diffusivity, and Perfusion," *Biomed. Sci. Instrum.*, 29: 435 - 442, 1993.

Table 1. Model Parameters

	Inner Radius (m)	Outer Radius (m)	Thermal Conductivity (W/m-˚C)	Density (kg/m^3)	Specific Heat (J/kg-˚C)	Microwave Attenuation Constant, β (m^{-1})
Catheter	2.286 x 10^{-3}	2.54 x 10^{-3}	0.175	1100	2010	–
Gel	2.54 x 10^{-3}	30.0 x 10^{-3}	0.56	1030	4180	41.284
Prostate	2.54 x 10^{-3}	25.0 x 10^{-3}	0.522	1060	3621	41.284
Peripheral Tissue	25.0 x 10^{-3}	30.0 x 10^{-3}	0.522	1060	3621	41.284

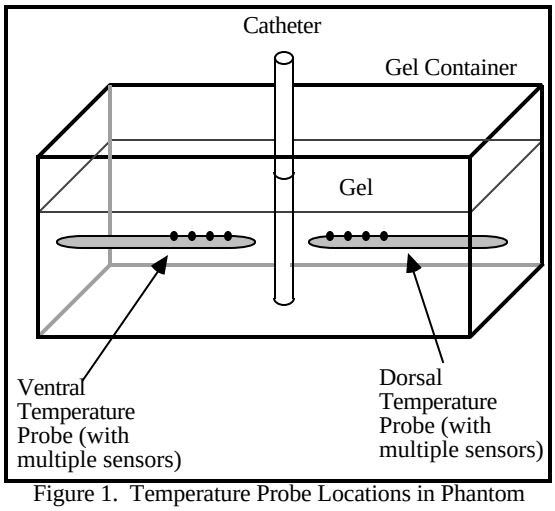

Figure 1. Temperature Probe Locations in Phantom

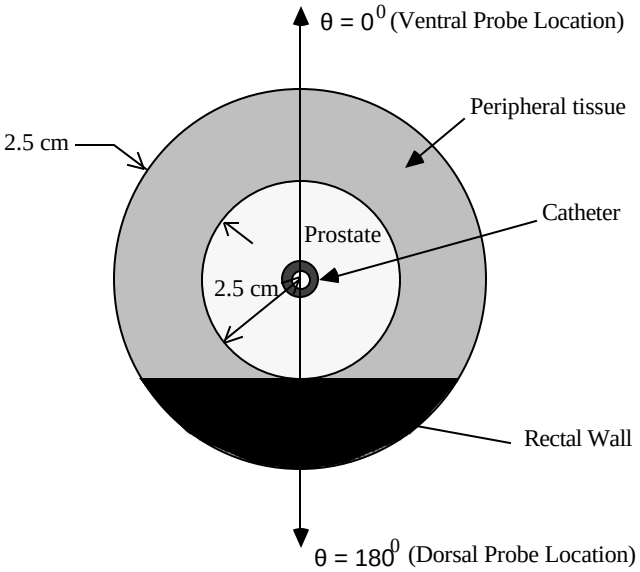

Figure 2. Model of Prostate Transverse Cross-Section